Sensorless DTC-SVM for Induction Motor Driven by a Matrix Converter Using a Parameter Estimation Strategy

Kyo-Beum Lee, *Member, IEEE*, and Frede Blaabjerg, *Fellow, IEEE*

***Abstract*—This paper presents a new direct torque controlled space vector modulated method to improve the sensorless performance of matrix converter drives using a parameter estimation scheme. The flux and torque error are geometrically combined in a new flux leakage vector to make a stator command voltage vector in a deadbeat manner. A new sensorless method of estimating the rotor speed, flux, stator resistance, and rotor resistance is derived and verified with experimental results. Common terms in the error dynamics are utilized to find a simpler error model involving some auxiliary variables. Using this error model, the state estimation problem is converted into a parameter estimation problem assuming the rotor speed is constant. The proposed adaptive schemes are determined so that the whole system is stable in the sense of Lyapunov. The effectiveness of the proposed algorithm is verified by experiments.**

***Index Terms*—AC–AC power conversion, AC motor drives, observers.**

I. Introduction

THE INDUCTION motor drive fed by a matrix converter is superior to the conventional inverter because it does not have bulky dc-link capacitors with limited lifetime and offers bidirectional power flow capability, sinusoidal input/output currents, and an adjustable input power factor. Furthermore, because of the high integration, the matrix converter topology is recommended for extreme temperatures and critical volume/weight applications [1], [2]. The direct torque control (DTC) scheme for matrix converter drives was initially presented in [3]. The generation of the voltage vectors required to implement the DTC of induction motors under a unity input power factor constraint was allowed. However, the DTC scheme using a switching table has some fatal drawbacks. Switching frequency varies according to the motor speed and the hysteresis bands of torque and flux, a large torque ripple is generated in a low speed range because of the small back electromotive force (EMF) of the induction motor, and high control sampling time is required to achieve good performance [4]. Although several methods to solve these problems have been presented [5]–[7], these methods are designed for a conventional inverter drive system. On the contrary, research results to solve these problems for matrix converter drives have not been reported in the literature.

To realize high performance sensorless control of induction motor drives, several observer-based methods are very attractive and give good performance in a large speed range [8]–[12]. Observation algorithms make use of the analytic model of the induction motor and allow the estimation of both rotor speed and flux from the stator currents and voltages. These are relatively simple to implement. Among the observer-based methods, the extended Kalman filter appeared to be the ultimate solution for speed sensorless drives [8] for a certain period. Unfortunately, this stochastic observer has some inherent disadvantages such as the influence of noise characteristic, the computational burden, and the absence of design and tuning criteria. This has led to a renewed interest in deterministic approaches, where the structure of the standard Luenberger observer for a linear system is enhanced to permit the simultaneous estimation of rotor flux and speed [9]–[11]. In the schemes by Kuboda *et al.* [9]–[11] the observer gain matrix is related to the immeasurable rotor speed and the observer needs motor parameter estimation to obtain good sensorless performance in the low speed operation. This makes the observer inappropriate for practical applications. There are other schemes which use a time-scale separation property of the induction motor model [12]. In these schemes, however, coordinate transformations involved are functions of the rotor speed.

In this paper, a new stable method of estimating rotor speed, flux, stator resistance, and rotor resistance has been derived. Common terms in the error dynamics are utilized to find a simpler error model involving some auxiliary variables. Using this error model, the state estimation problem is converted into a parameter estimation problem assuming that the rotor speed is constant. The speed and parameter adaptation laws are designed so that the estimated stator currents converge to the measured ones. Some stability properties are given on the basis of Lyapunov analysis. The proposed control scheme of the sensorless DTC for induction motor drives using a matrix converter is shown in Fig. 1. The scheme consists of a flux deadbeat controller with overmodulation strategy, displacement angle calculator, indirect space vector modulation (ISVM), the proposed estimator for speed, parameter estimation, and compensation of nonlinearities of the matrix converter [14]. The

Manuscript received March 28, 2006; revised December 9, 2006.

K.-B. Lee was with the Division of Electronics and Information Engineering, Chonbuk National University, Jeonju 561-756, Korea. He is now with the School of Electrical and Computer Engineering, Ajou University, Suwon 443-749, Korea (e-mail: kyl@chonbuk.ac.kr).

F. Blaabjerg is with the Institute of Energy Technology, Aalborg University, 9220 Aalborg East, Denmark (e-mail: fbl@iet.aau.dk).

Color versions of one or more of the figures in this paper are available online at http://ieeexplore.ieee.org.

Digital Object Identifier 10.1109/TIE.2007.911940

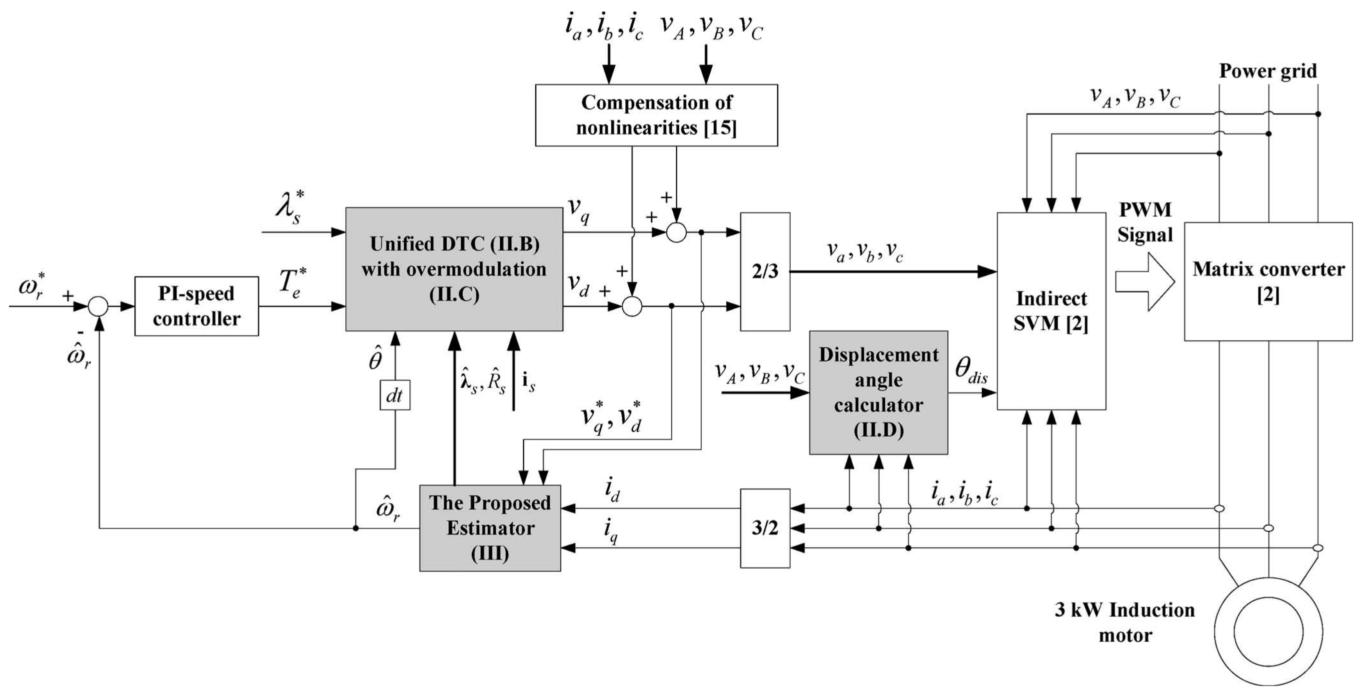

Fig. 1. Proposed sensorless DTC-SVM for matrix converter drives.

effectiveness of the proposed scheme is demonstrated through experimental results.

II. Novel Unified DTC-SVM for Matrix Converter Drives

The basic DTC method for matrix converter drives allows for the generation of the voltage vectors required to implement the DTC of the induction motor under a unity input power factor constraint. However, the switching frequency varies according to the motor speed and the hysteresis bands of torque and flux, a large torque ripple is generated in a low speed range because of the small back EMF of an induction motor, and high control sampling time is required to achieve good performance [4]. To cope with these problems, a new DTC is proposed. The proposed scheme consists of a deadbeat controller with an overmodulation strategy and a detector of the input voltage angle.

A. Induction Motor Equations

An induction motor can be described in a general reference frame, denoted by the subscript "g," by the following flux and voltage equations:

$$\begin{aligned} \boldsymbol{\lambda}_{\rm gs} &= L_{\rm s}\mathbf{i}_{\rm gs} + L_{\rm m}\mathbf{i}_{\rm gr} \\ \boldsymbol{\lambda}_{\rm gr} &= L_{\rm m}\mathbf{i}_{\rm gs} + L_{\rm r}\mathbf{i}_{\rm gr} \end{aligned} \tag{1}$$

$$\begin{aligned} \mathbf{v}_{\rm gs} &= R_{\rm s}\mathbf{i}_{\rm gs} + \frac{d}{dt}\boldsymbol{\lambda}_{\rm gs} + j\omega_{\rm g}\boldsymbol{\lambda}_{\rm gs} \\ 0 &= R_{\rm r}\mathbf{i}_{\rm gr} + \frac{d}{dt}\boldsymbol{\lambda}_{\rm gr} + j(\omega_{\rm g} - \omega_{\rm r})\boldsymbol{\lambda}_{\rm gr} \end{aligned} \tag{2}$$

where $\boldsymbol{\lambda}_{\rm gs}$ and $\boldsymbol{\lambda}_{\rm gr}$ are the stator and rotor flux vectors in a general reference frame, $\mathbf{i}_{\rm gs}$ and $\mathbf{i}_{\rm gr}$ are the stator and rotor current vectors in a general reference frame, $\mathbf{v}_{\rm gs}$ is the stator voltage vector in a general reference frame, $\omega_{\rm g}$ is the reference frame speed, and $\omega_{\rm r}$ is the rotor speed.

If the referred values are used with a referring factor $a = L_{\rm m}/L_{\rm r}$ to remove rotor leakage inductance, the flux and voltage equations can be rewritten by

$$\begin{aligned} \boldsymbol{\lambda}_{\rm gs} &= L_{\rm s}\mathbf{i}_{\rm gs} + L'_{\rm r}\mathbf{i}'_{\rm gr} \\ \lambda'_{\rm gr} &= L'_{\rm r}\mathbf{i}_{\rm gs} + L'_{\rm r}\mathbf{i}'_{\rm gr} \end{aligned} \tag{3}$$

$$\begin{aligned} \mathbf{v}_{\rm gs} &= R_{\rm s}\mathbf{i}_{\rm gs} + \frac{d}{dt}\boldsymbol{\lambda}_{\rm gs} + j\omega_{\rm g}\boldsymbol{\lambda}_{\rm gs} \\ 0 &= R'_{\rm r}\mathbf{i}'_{\rm gr} + \frac{d}{dt}\lambda'_{\rm gr} + j(\omega_{\rm g} - \omega_{\rm r})\lambda'_{\rm gr} \end{aligned} \tag{4}$$

where $\boldsymbol{\lambda}'_{\rm gr} = a\lambda_{\rm gr}$, $\mathbf{i}'_{\rm gr} = (1/a)\mathbf{i}_{\rm gr}$, $L'_{\rm m} = a^2 L_{\rm r}$, and $R'_{\rm r} = a^2 R_{\rm r}$.

Here, the leakage flux vector $\boldsymbol{\lambda}_{\rm g\sigma}$ is defined as follows:

$$\boldsymbol{\lambda}_{\rm g\sigma} = L_\sigma \mathbf{i}_{\rm gs} = \boldsymbol{\lambda}_{\rm gs} - \boldsymbol{\lambda}'_{\rm gr} \tag{5}$$

where $L_\rho = \sigma L_{\rm s} = L_{\rm s} - L'_{\rm r}$.

The leakage flux vector $\boldsymbol{\lambda}_{\rm g\sigma}$ can be calculated from current measurement with the knowledge of L_ρ. Rearranging the equations, the following state equation is obtained:

$$\begin{aligned} \frac{d}{dt}\begin{bmatrix} \boldsymbol{\lambda}_{\rm gs} \\ \boldsymbol{\lambda}'_{\rm gr} \end{bmatrix} &= \begin{bmatrix} -(1/\tau'_{\rm s})\mathbf{I} - \omega_{\rm g}\mathbf{J} & (1/\tau'_{\rm s})\mathbf{I} \\ ((1-\sigma)/\tau'_{\rm r})\mathbf{I} & -(1/\tau'_{\rm r})\mathbf{I} - (\omega_{\rm g} - \omega_{\rm r})\mathbf{J} \end{bmatrix} \\ &\quad \times \begin{bmatrix} \boldsymbol{\lambda}_{\rm gs} \\ \boldsymbol{\lambda}'_{\rm gr} \end{bmatrix} + \begin{bmatrix} \mathbf{I} \\ 0 \end{bmatrix} \mathbf{v}_{\rm gs} \\ &= \mathbf{A}_{\rm g}\mathbf{x}_{\rm g} + \mathbf{B}\mathbf{v}_{\rm gs} \end{aligned} \tag{6}$$

$$\boldsymbol{\lambda}_{\rm g\sigma} = [\mathbf{I} \quad -\mathbf{I}]\mathbf{x}_{\rm g} = \mathbf{C}\mathbf{x}_{\rm g} \tag{7}$$

where $\tau'_{\rm s} = L_{\rm r}/R_{\rm s} = \sigma L_{\rm s}/R_{\rm s}$, $\tau'_{\rm r} = \sigma\tau_{\rm r}$, $\mathbf{I} = \begin{bmatrix} 1 & 0 \\ 0 & 1 \end{bmatrix}$, and $\mathbf{J} = \begin{bmatrix} 0 & -1 \\ 1 & 0 \end{bmatrix}$.

By introducing another set of space vectors $\tilde{\mathbf{x}}_{\rm g}$, defined by

$$\tilde{\mathbf{x}}_{\rm g} = \begin{bmatrix} \boldsymbol{\lambda}_{\rm gs} \\ \boldsymbol{\lambda}_{\rm g\sigma} \end{bmatrix} = \begin{bmatrix} \mathbf{I} & 0 \\ \mathbf{I} & -\mathbf{I} \end{bmatrix} \mathbf{x}_{\rm g}, \tag{8}$$

the stator equation can be written as

$$\frac{d}{dt}\tilde{\mathbf{x}}_{\rm g} = \begin{bmatrix} -\omega_{\rm g}\mathbf{J} & -\left(1/\tau'_{\rm s}\right)\mathbf{I} \\ (1/\tau_{\rm r})\mathbf{I} - \omega_{\rm r}\mathbf{J} & -\left(1/\tau'_{\rm s} + 1/\tau'_{\rm r}\right)\mathbf{I} - (\omega_{\rm g} - \omega_{\rm r})\mathbf{J} \end{bmatrix} \times \begin{bmatrix} \boldsymbol{\lambda}_{\rm gs} \\ \boldsymbol{\lambda}_{\rm g\sigma} \end{bmatrix} + \begin{bmatrix} \mathbf{I} \\ 0 \end{bmatrix} \mathbf{v}_{\rm gs}. \tag{9}$$

B. Novel Unified DTC Using a Deadbeat Scheme

Since the voltage drops by stator and rotor resistances are much smaller than the input voltages, (9) can be approximated in the stator flux reference frame as

$$\frac{d}{dt}\tilde{\mathbf{x}}_{\rm dq} = \begin{bmatrix} -\omega_{\rm e}\mathbf{J} & 0 \\ -\omega_{\rm r}\mathbf{J} & -(\omega_{\rm e} - \omega_{\rm r})\mathbf{J} \end{bmatrix} \tilde{\mathbf{x}}_{\rm dq} + \begin{bmatrix} \mathbf{I} \\ \mathbf{I} \end{bmatrix} \mathbf{v}_{\rm dqs} \tag{10}$$

where $\omega_{\rm e}$ is the angular speed of the stator flux vector.

This is much simpler than (9) since the system matrix contains no time-constant related elements. It follows from (10) that:

$$\begin{aligned} \frac{d}{dt}|\lambda_{\rm s}| &= v_{\rm ds} \\ 0 &= -\omega_{\rm e}|\lambda_{\rm s}| + v_{\rm qs} \\ \frac{d}{dt}\lambda_{\rm d\sigma} &= (\omega_{\rm e} - \omega_{\rm r})\lambda_{\rm q\sigma} + v_{\rm ds} \\ \frac{d}{dt}\lambda_{\rm q\sigma} &= -\omega_{\rm r}|\lambda_{\rm s}| - (\omega_{\rm e} - \omega_{\rm r})\lambda_{\rm d\sigma} + v_{\rm qs}. \end{aligned} \tag{11}$$

The flux-linkage space vectors are shown in Fig. 2. The electromagnetic torque can be expressed in terms of the flux components as

$$T_{\rm e} = \frac{3}{2}p|\lambda_{\rm s}|\,|\lambda'_{\rm r}|\sin\delta/L_\sigma = \frac{3}{2}p|\lambda_{\rm s}|\lambda_{\rm q\sigma}/L_\sigma. \tag{12}$$

Ideally, a deadbeat controller would establish zero torque and flux error within one sampling period, $t_{\rm sp}$. In a digital control system, the controller algorithm computes the required stator voltage vector such that the torque and flux error are eliminated in the next sampling instant. Referring to (11) and (12), the required stator voltage in discrete form can be obtained [16]

$$\begin{aligned} v^*_{{\rm ds},k+1} &= \frac{|\lambda_{{\rm s},k}|^* - |\lambda_{{\rm s},k}|}{t_{\rm sp}} \\ v^*_{{\rm qs},k+1} &= \frac{|\lambda_{{\rm s},k}|^*/\lambda_{{\rm dr},k}\left(\lambda^*_{{\rm q}\sigma,k} - \lambda_{{\rm q}\sigma,k}\right)}{t_{\rm sp}} + \omega_{{\rm r},k}|\lambda_{{\rm s},k}| \end{aligned} \tag{13}$$

where $\lambda^*_{{\rm q}\sigma,k} = (L_\sigma T^*_{{\rm e},k})/((3/2)p|\lambda_{{\rm s},k}|^*)$.

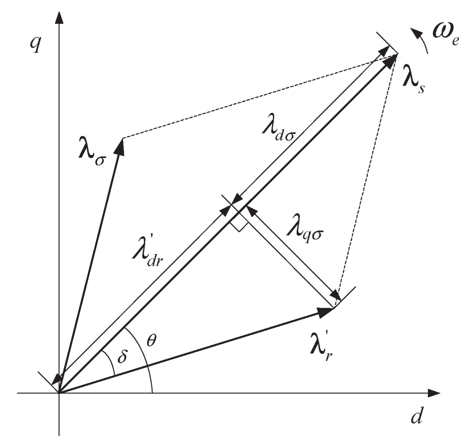

Fig. 2. Flux-leakage space vectors for induction motor.

C. Improvement of Transient Response

Without energy storage in the matrix converter, the output voltages have to be generated from the input voltage. This means that the desired output voltages have to fit within the enveloping curve of the input voltage system at any time. Fig. 3 shows that the minimum of the enveloping curve equals 0.866 times the peak input line voltage. This value for sinusoidal operation is a theoretical limit because step-up operation is not possible without changing the modulation method.

From (11) and (12), the change in electromagnetic torque during one sampling period can be described as

$$\begin{aligned} \Delta T_{{\rm e},k+1} &= T_{{\rm e},k+1} - T_{{\rm e},k} \\ &= \frac{3}{2L_\sigma}p\{\lambda_{{\rm q}\sigma,k}v_{{\rm max,ds},k} + \lambda'_{\rm dr}(v_{{\rm max,qs},k} - \omega_{\rm r}|\lambda_{\rm s}|)\}t_{\rm sp}. \end{aligned} \tag{14}$$

However, the largest output magnitude can be expected if the edges of the hexagon for 60° are used instead of the circular locus diagram as shown in Fig. 4. When the torque error, $\Delta T_{\rm e} = T^*_{\rm e} - T_{\rm e}$, exceeds the maximum allowable change of electromagnetic torque value in (14), an alternative torque control method must be derived instead of a flux deadbeat control scheme. To cope with this problem, an overmodulation control scheme for matrix converter drives is proposed. In this way, the drive combines advantages of the smooth steady-state operation and rapid transient response to the control reference.

D. Detection of Input Voltage Angle

To implement the ISVM, the input reference current vector is given by the input voltage vector for an instantaneous unitary power factor. Under balanced conditions, the angular velocity and the magnitude of the input voltage vector is constant. In this situation, the determination of the input current reference angle is quite straightforward. Unfortunately, with unbalanced supply voltages, the negative sequence component of the voltage causes variation in magnitude and angular velocity of the input voltage vector. In this case, a different modulation strategy should be considered (see Fig. 5).

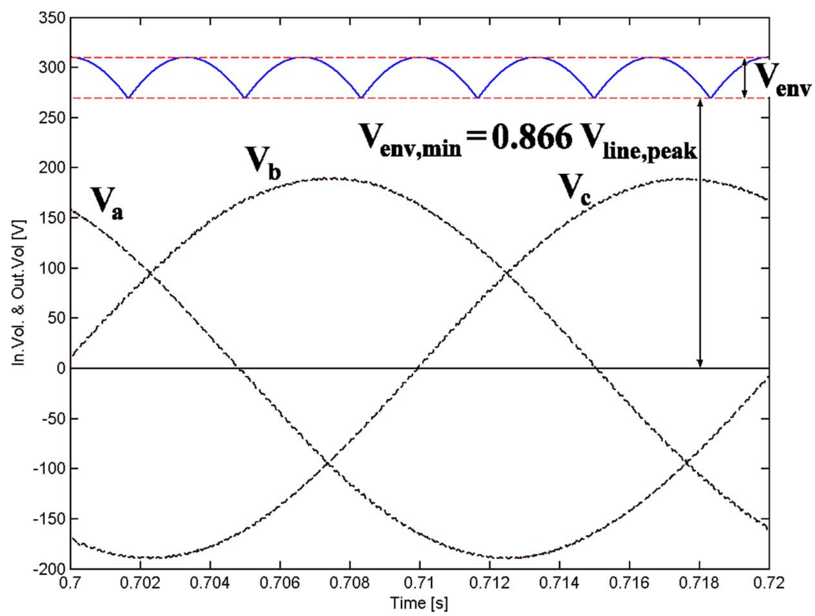

Fig. 3. Enveloping curve of the input voltages and output phase voltages.

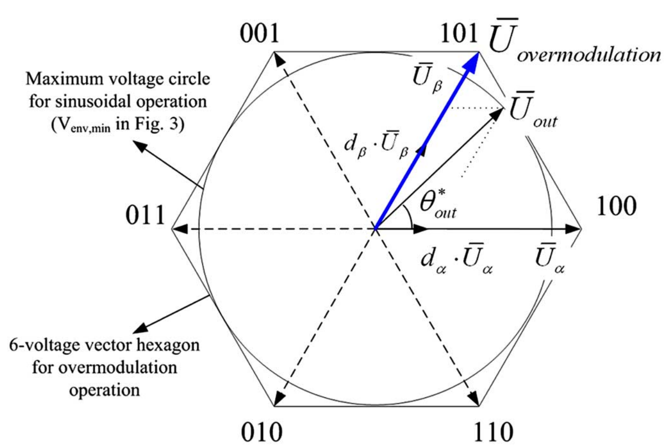

Fig. 4. Output voltage vectors using ISVM in a matrix converter (inversion stage).

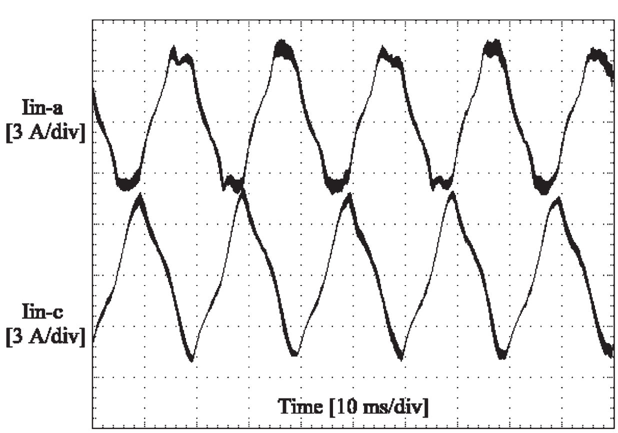

Fig. 5. Input phase currents in a matrix converter (under 20% input voltage unbalanced condition).

A block diagram of the proposed detection of input voltage angle is presented in Fig. 6. The three-phase input voltages (v_a, v_b, v_c) are converted into the values of d- and q-axis voltages in the synchronous frame as

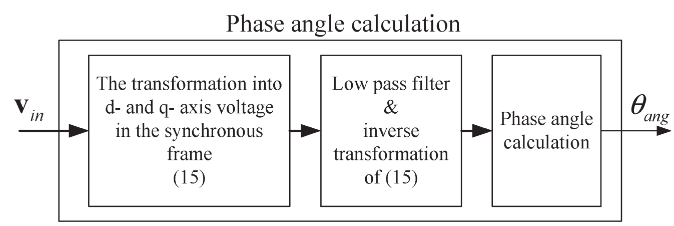

Fig. 6. Block diagram of the input voltage angle calculation.

$$\begin{bmatrix} v_d^s \\ v_q^s \end{bmatrix} = \frac{2}{3}\begin{bmatrix} 1 & -1/2 & -1/2 \\ 0 & \sqrt{2}/3 & -\sqrt{2}/3 \end{bmatrix}\begin{bmatrix} v_a \\ v_b \\ v_c \end{bmatrix}$$

$$\begin{bmatrix} v_d^e \\ v_q^e \end{bmatrix} = \begin{bmatrix} \cos\hat{\theta} & -\sin\hat{\theta} \\ \sin\hat{\theta} & \cos\hat{\theta} \end{bmatrix}\begin{bmatrix} v_d^s \\ v_q^s \end{bmatrix}. \tag{15}$$

In (15), v_q^e is set to zero for the unity power factor control and v_d^e is constant under the balanced input voltage conditions. However, under the unbalanced input voltage conditions, v_q^e and v_d^e cannot be kept constant because they both contain the second-order harmonic component by the negative sequence voltage and degrade input power quality. To alleviate this problem, they can be separated into a dc part and an ac part by simple low-pass filters, followed by a reconstruction of the virtual balanced input voltages using only the dc part. By using these reconstructed voltages, a constant magnitude input voltage vector that rotates at a constant angular velocity can be developed and the result can be seen in Fig. 7.

III. Estimator Design for Speed and Parameters

The previous discussed observer estimates the motor speed except zero-frequency condition, when the observer gain is properly designed. However, the gain should be reselected for the regenerating operation [9], [10]. In this section, a new

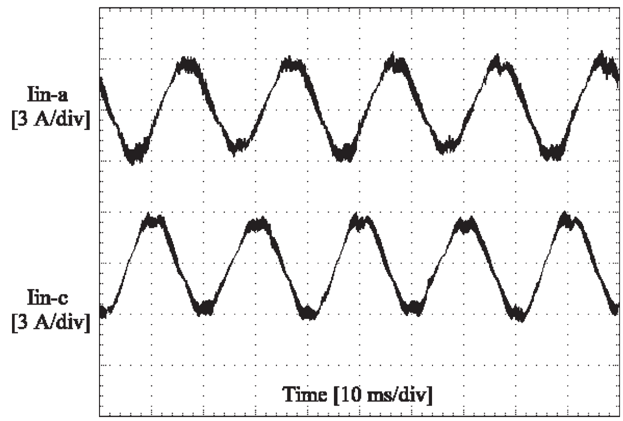

Fig. 7. Input phase currents in a matrix converter (under 20% input voltage unbalanced condition with simple compensation).

estimator design method is explained. The proposed design method is independent of the operating condition. In addition, the stator resistance can also be estimated within the same framework.

A. Induction Motor Model for Estimator Design

An induction motor can be described by the following state equations in the stationary reference frame:

$$\begin{aligned}
\dot{i}_{\mathrm{ds}} &= -\frac{L_{\mathrm{m}}}{\sigma L_{\mathrm{s}}}\left(-\frac{R_{\mathrm{r}}}{L_{\mathrm{r}}}\lambda_{\mathrm{dr}} - \omega_{\mathrm{r}}\lambda_{\mathrm{qr}} + \frac{L_{\mathrm{m}}}{\tau_{\mathrm{r}}} i_{\mathrm{ds}}\right) - \frac{R_{\mathrm{s}}}{\sigma L_{\mathrm{s}}} i_{\mathrm{ds}} + \frac{1}{\sigma L_{\mathrm{s}}} v_{\mathrm{ds}} \\
\dot{i}_{\mathrm{qs}} &= -\frac{L_{\mathrm{m}}}{\sigma L_{\mathrm{s}}}\left(-\frac{R_{\mathrm{r}}}{L_{\mathrm{r}}}\lambda_{\mathrm{qr}} + \omega_{\mathrm{r}}\lambda_{\mathrm{dr}} + \frac{L_{\mathrm{m}}}{\tau_{\mathrm{r}}} i_{\mathrm{qs}}\right) - \frac{R_{\mathrm{s}}}{\sigma L_{\mathrm{s}}} i_{\mathrm{qs}} + \frac{1}{\sigma L_{\mathrm{s}}} v_{\mathrm{qs}} \\
\dot{\lambda}_{\mathrm{dr}} &= -\frac{R_{\mathrm{r}}}{L_{\mathrm{r}}}\lambda_{\mathrm{dr}} - \omega_{\mathrm{r}}\lambda_{\mathrm{qr}} + L_{\mathrm{m}}\frac{R_{\mathrm{r}}}{L_{\mathrm{r}}} i_{\mathrm{ds}} \\
\dot{\lambda}_{\mathrm{qr}} &= -\frac{R_{\mathrm{r}}}{L_{\mathrm{r}}}\lambda_{\mathrm{qr}} + \omega_{\mathrm{r}}\lambda_{\mathrm{dr}} + L_{\mathrm{m}}\frac{R_{\mathrm{r}}}{L_{\mathrm{r}}} i_{\mathrm{qs}}.
\end{aligned} \tag{16}$$

On the basis of this model, a new method of estimating rotor speed, stator resistance and flux is proposed. It is assumed that only the stator currents and voltages are measurable and all system parameters are known.

B. Design of Speed and Flux Estimator

To obtain a speed and flux estimator, we proceed as in [14]. The estimator, which observes the rotor speed and the rotor flux together, is written by the following equation:

$$\begin{aligned}
\dot{\hat{i}}_{\mathrm{ds}} &= -\frac{L_{\mathrm{m}}}{\sigma L_{\mathrm{s}}}\left(-\frac{R_{\mathrm{r}}}{L_{\mathrm{r}}}\hat{\lambda}_{\mathrm{dr}} - \hat{\omega}_{\mathrm{r}}\hat{\lambda}_{\mathrm{qr}} + L_{\mathrm{m}}\frac{R_{\mathrm{r}}}{L_{\mathrm{r}}} i_{\mathrm{ds}}\right) + \frac{1}{\sigma L_{\mathrm{s}}} v_{\mathrm{ds}} - u_{\mathrm{ds}} \\
\dot{\hat{i}}_{\mathrm{qs}} &= -\frac{L_{\mathrm{m}}}{\sigma L_{\mathrm{s}}}\left(-\frac{R_{\mathrm{r}}}{L_{\mathrm{r}}}\hat{\lambda}_{\mathrm{qr}} + \hat{\omega}_{\mathrm{r}}\hat{\lambda}_{\mathrm{dr}} + L_{\mathrm{m}}\frac{R_{\mathrm{r}}}{L_{\mathrm{r}}} i_{\mathrm{qs}}\right) + \frac{1}{\sigma L_{\mathrm{s}}} v_{\mathrm{qs}} - u_{\mathrm{qs}} \\
\dot{\hat{\lambda}}_{\mathrm{dr}} &= -\frac{R_{\mathrm{r}}}{L_{\mathrm{r}}}\hat{\lambda}_{\mathrm{dr}} - \hat{\omega}_{\mathrm{r}}\hat{\lambda}_{\mathrm{qr}} + L_{\mathrm{m}}\frac{R_{\mathrm{r}}}{L_{\mathrm{r}}} i_{\mathrm{ds}} \\
\dot{\hat{\lambda}}_{\mathrm{qr}} &= -\frac{R_{\mathrm{r}}}{L_{\mathrm{r}}}\hat{\lambda}_{\mathrm{qr}} + \hat{\omega}_{\mathrm{r}}\hat{\lambda}_{\mathrm{dr}} + L_{\mathrm{m}}\frac{R_{\mathrm{r}}}{L_{\mathrm{r}}} i_{\mathrm{qs}}
\end{aligned} \tag{17}$$

where u_{ds} and u_{qs} are the observer compensation voltages to be designed. Let us introduce the error variables

$$\begin{aligned}
\tilde{i}_{\mathrm{ds}} &= i_{\mathrm{ds}} - \hat{i}_{\mathrm{ds}}, \quad \tilde{i}_{\mathrm{qs}} = i_{\mathrm{qs}} - \hat{i}_{\mathrm{qs}} \\
\tilde{\lambda}_{\mathrm{dr}} &= \lambda_{\mathrm{dr}} - \hat{\lambda}_{\mathrm{dr}}, \quad \tilde{\lambda}_{\mathrm{qr}} = \lambda_{\mathrm{qr}} - \hat{\lambda}_{\mathrm{qr}} \\
\tilde{\omega}_{\mathrm{r}} &= \omega_{\mathrm{r}} - \hat{\omega}_{\mathrm{r}}.
\end{aligned} \tag{18}$$

It follows from (16)–(18) that:

$$\begin{aligned}
\dot{\tilde{i}}_{\mathrm{ds}} &= -\frac{L_{\mathrm{m}}}{\sigma L_{\mathrm{s}} L_{\mathrm{r}}}\left\{-\frac{R_{\mathrm{r}}}{L_{\mathrm{r}}}\tilde{\lambda}_{\mathrm{dr}} - (\omega_{\mathrm{r}}\tilde{\lambda}_{\mathrm{qr}} + \hat{\lambda}_{\mathrm{qr}}\tilde{\omega}_{\mathrm{r}})\right\} + u_{\mathrm{ds}} \\
\dot{\tilde{i}}_{\mathrm{qs}} &= -\frac{L_{\mathrm{m}}}{\sigma L_{\mathrm{s}} L_{\mathrm{r}}}\left\{-\frac{R_{\mathrm{r}}}{L_{\mathrm{r}}}\tilde{\lambda}_{\mathrm{qr}} + (\omega_{\mathrm{r}}\tilde{\lambda}_{\mathrm{dr}} + \hat{\lambda}_{\mathrm{dr}}\tilde{\omega}_{\mathrm{r}})\right\} + u_{\mathrm{qs}} \\
\dot{\tilde{\lambda}}_{\mathrm{dr}} &= -\frac{R_{\mathrm{r}}}{L_{\mathrm{r}}}\tilde{\lambda}_{\mathrm{dr}} - (\omega_{\mathrm{r}}\tilde{\lambda}_{\mathrm{qr}} + \hat{\lambda}_{\mathrm{qr}}\tilde{\omega}_{\mathrm{r}}) \\
\dot{\tilde{\lambda}}_{\mathrm{qr}} &= -\frac{R_{\mathrm{r}}}{L_{\mathrm{r}}}\tilde{\lambda}_{\mathrm{qr}} + (\omega_{\mathrm{r}}\tilde{\lambda}_{\mathrm{dr}} + \hat{\lambda}_{\mathrm{dr}}\tilde{\omega}_{\mathrm{r}}).
\end{aligned} \tag{19}$$

The adaptation law for ω_{r} and the design voltage vector $\mathbf{u}_{\mathrm{s}} = [u_{\mathrm{ds}} \quad u_{\mathrm{qs}}]^{\mathrm{T}}$ should be designed so that $\tilde{i}_{\mathrm{ds}}$ and $\tilde{i}_{\mathrm{qs}}$ tend asymptotically to zero. However, deriving the design function directly from (19) is not straightforward due to the unknown state error terms multiplied by an unknown parameter such as $\omega\tilde{\lambda}_{\mathrm{dr}}$. To cope with the problem, the new variables are introduced

$$z_{\mathrm{ds}} = \tilde{i}_{\mathrm{ds}} + \frac{L_{\mathrm{m}}}{\sigma L_{\mathrm{s}} L_{\mathrm{r}}}\tilde{\lambda}_{\mathrm{dr}}, \quad z_{\mathrm{qs}} = \tilde{i}_{\mathrm{qs}} + \frac{L_{\mathrm{m}}}{\sigma L_{\mathrm{s}} L_{\mathrm{r}}}\tilde{\lambda}_{\mathrm{qr}}. \tag{20}$$

From (19) and (20), we obtain

$$\dot{z}_{\mathrm{ds}} = v_{\mathrm{ds}}, \quad \dot{z}_{\mathrm{qs}} = v_{\mathrm{qs}} \tag{21}$$

where the initial conditions are unknown. This is an advantage over (19) in which the dynamics of the unknown variables, $(\tilde{\lambda}_{\mathrm{dr}}, \tilde{\lambda}_{\mathrm{qr}})$ are not known. This justified the introduction of the variables $(z_{\mathrm{ds}}, z_{\mathrm{qs}})$.

Define the first-order filters

$$\dot{\zeta}_{\mathrm{ds}} = v_{\mathrm{ds}}, \quad \dot{\zeta}_{\mathrm{qs}} = v_{\mathrm{qs}} \tag{22}$$

so that

$$\frac{L_{\mathrm{m}}}{\sigma L_{\mathrm{s}} L_{\mathrm{r}}}\tilde{\lambda}_{\mathrm{dr}} = A - \zeta_{\mathrm{ds}} - \tilde{i}_{\mathrm{ds}}, \quad \frac{L_{\mathrm{m}}}{\sigma L_{\mathrm{s}} L_{\mathrm{r}}}\tilde{\lambda}_{\mathrm{qr}} = B - \zeta_{\mathrm{qs}} - \tilde{i}_{\mathrm{qs}} \tag{23}$$

with A and B unknown constants depending on initial conditions

$$A = \tilde{i}_{\mathrm{ds}}(0) + \frac{L_{\mathrm{m}}}{\sigma L_{\mathrm{s}} L_{\mathrm{r}}}\tilde{\lambda}_{\mathrm{dr}}(0), \quad B = \tilde{i}_{\mathrm{qs}}(0) + \frac{L_{\mathrm{m}}}{\sigma L_{\mathrm{s}} L_{\mathrm{r}}}\tilde{\lambda}_{\mathrm{qr}}(0). \tag{24}$$

Substituting the expressions $(L_{\mathrm{m}}/\sigma L_{\mathrm{s}} L_{\mathrm{r}})\tilde{\lambda}_{\mathrm{dr}}$ and $(L_{\mathrm{m}}/\sigma L_{\mathrm{s}} L_{\mathrm{r}})\tilde{\lambda}_{\mathrm{dr}}$ given by (23) into the first two equations in (19) we obtain

$$\begin{aligned}\dot{\tilde{i}}_{\rm ds} =& \frac{R_{\rm r}}{L_{\rm r}}\tilde{i}_{\rm ds} - \omega_{\rm r}\tilde{i}_{\rm qs} + \frac{L_{\rm m}}{\sigma L_{\rm s}L_{\rm r}}\hat{\lambda}_{\rm qr}\tilde{\omega}_{\rm r}\\ &+ \frac{R_{\rm r}}{L_{\rm r}}A + \omega_{\rm r}B + \frac{R_{\rm r}}{L_{\rm r}}\zeta_{\rm ds} + \omega_{\rm r}\zeta_{\rm qs} + u_{\rm ds}\\ \dot{\tilde{i}}_{\rm qs} =& \omega_{\rm r}\tilde{i}_{\rm ds} - \frac{R_{\rm r}}{L_{\rm r}}\tilde{i}_{\rm qs} - \frac{L_{\rm m}}{\sigma L_{\rm s}L_{\rm r}}\hat{\lambda}_{\rm dr}\tilde{\omega}_{\rm r}\\ &+ \frac{R_{\rm r}}{L_{\rm r}}B - \omega_{\rm r}A - \omega_{\rm r}\zeta_{\rm qs} + \frac{R_{\rm r}}{L_{\rm r}}\zeta_{\rm qs} + u_{\rm qs}.\end{aligned} \tag{25}$$

Now we define $u_{\rm ds}$ and $u_{\rm qs}$ to partially compensate some of the terms in the right-hand side of the two equations in (25)

$$\begin{aligned}u_{\rm ds} &= -\left(\rho_{\rm ds}\tilde{i}_{\rm ds} + \frac{R_{\rm r}}{L_{\rm r}}\zeta_{\rm ds} + \hat{\omega}_{\rm r}\zeta_{\rm qs} + \hat{\xi}_{\rm ds}\right)\\ u_{\rm qs} &= -\left(\rho_{\rm qs}\tilde{i}_{\rm qs} + \frac{R_{\rm r}}{L_{\rm r}}\zeta_{\rm qs} - \hat{\omega}_{\rm r}\zeta_{\rm ds} + \hat{\xi}_{\rm qs}\right)\end{aligned} \tag{26}$$

where $\rho_{\rm ds}$ and $\rho_{\rm qs}$ are positive design parameters, and $\hat{\xi}_{\rm ds}$ and $\hat{\xi}_{\rm qs}$ are estimates of the term, $(R_{\rm r}/L_{\rm r})A + \omega_{\rm r}B$ and $(R_{\rm r}/L_{\rm r})B - \omega_{\rm r}A$ in (25).

Substituting (26) into (25), the error dynamics become

$$\begin{aligned}\dot{\tilde{i}}_{\rm ds} &= -\left(\rho_{\rm ds}+\frac{R_{\rm r}}{L_{\rm r}}\right)\tilde{i}_{\rm ds} - \omega_{\rm r}\tilde{i}_{\rm qs} + \tilde{\omega}_{\rm r}\left(\zeta_{\rm qs}+\frac{L_{\rm m}}{\sigma L_{\rm s}L_{\rm r}}\hat{\lambda}_{\rm qr}\right) + \tilde{\xi}_{\rm ds}\\ \dot{\tilde{i}}_{\rm qs} &= \omega_{\rm r}\tilde{i}_{\rm ds} - \left(\rho_{\rm qs}+\frac{R_{\rm r}}{L_{\rm r}}\right)\tilde{i}_{\rm qs} - \tilde{\omega}_{\rm r}\left(\zeta_{\rm ds}+\frac{L_{\rm m}}{\sigma L_{\rm s}L_{\rm r}}\hat{\lambda}_{\rm qr}\right) + \tilde{\xi}_{\rm qs}.\end{aligned} \tag{27}$$

Consider the Lyapunov function

$$V = \frac{1}{2}\left(\tilde{i}_{\rm ds}^2 + \tilde{i}_{\rm qs}^2 + \frac{1}{\gamma_1}\tilde{\omega}_{\rm r}^2 + \frac{1}{\gamma_2}\tilde{\xi}_{\rm ds}^2 + \frac{1}{\gamma_3}\tilde{\xi}_{\rm qs}^2\right) \tag{28}$$

where γ_1, γ_2, and γ_3 are positive design parameters.

Its time derivative is

$$\begin{aligned}\dot{V} =& -\left(\rho_{\rm ds} + \frac{R_{\rm r}}{L_{\rm r}}\right)\tilde{i}_{\rm ds}^2 - \left(\rho_{\rm qs} + \frac{R_{\rm r}}{L_{\rm r}}\right)\tilde{i}_{\rm qs}^2\\ &+ \tilde{\omega}_{\rm r}\left[\frac{1}{\gamma_1}\dot{\tilde{\omega}}_{\rm r} + \left\{\left(\zeta_{\rm qs} + \frac{L_{\rm m}}{\sigma L_{\rm s}L_{\rm r}}\hat{\lambda}_{\rm qr}\right)\tilde{i}_{\rm ds}\right.\right.\\ &\left.\left. - \left(\zeta_{\rm ds} + \frac{L_{\rm m}}{\sigma L_{\rm s}L_{\rm r}}\hat{\lambda}_{\rm dr}\right)\tilde{i}_{\rm qs}\right\}\right]\\ &+ \tilde{\xi}_{\rm ds}\left(\frac{1}{\gamma_2}\dot{\tilde{\xi}}_{\rm ds} + \tilde{i}_{\rm ds}\right) + \tilde{\xi}_{\rm qs}\left(\frac{1}{\gamma_3}\dot{\tilde{\xi}}_{\rm qs} + \tilde{i}_{\rm qs}\right).\end{aligned} \tag{29}$$

For speed estimation design, we now assume that speed is constant because the speed moves much more slowly than the other electrical variables, and propose the estimation laws as follows:

$$\begin{aligned}\hat{\omega}_{\rm r} &= \gamma_1\left\{\left(\zeta_{\rm qs}+\frac{L_{\rm m}}{\sigma L_{\rm s}L_{\rm r}}\hat{\lambda}_{\rm qr}\right)\tilde{i}_{\rm ds} - \left(\zeta_{\rm ds} + \frac{L_{\rm m}}{\sigma L_{\rm s}L_{\rm r}}\hat{\lambda}_{\rm dr}\right)\tilde{i}_{\rm qs}\right\}\\ \dot{\hat{\xi}}_{\rm ds} &= \gamma_2\tilde{i}_{\rm ds}\\ \dot{\hat{\xi}}_{\rm qs} &= \gamma_3\tilde{i}_{\rm qs}.\end{aligned} \tag{30}$$

It then follows that:

$$\dot{V} = -\left(\rho_{\rm ds} + \frac{R_{\rm r}}{L_{\rm r}}\right)\tilde{i}_{\rm ds}^2 - \left(\rho_{\rm qs} + \frac{R_{\rm r}}{L_{\rm r}}\right)\tilde{i}_{\rm qs}^2 \tag{31}$$

which guarantees the boundedness of all the variables and the convergence of $\tilde{i}_{\rm ds}$ and $\tilde{i}_{\rm qs}$ to zero under the assumption of constant speed. Note that as the speed estimate approaches the real speed, the flux estimation errors tend to zero.

C. Design of Stator Resistance Estimator

The stator resistance and rotor time constant are varied due to temperature changes during operation. In particular, the stator resistance, which has a deep effect on the performance of the low-speed operation in DTC, should be estimated under operation [11]. The proposed observer can be extended to include stator resistance estimation. When the stator resistance is treated as an unknown parameter of the observer, the estimation error of the stator current is rewritten from (27) and is given by the following equation:

$$\begin{aligned}\dot{\tilde{i}}_{\rm ds} =& -\left(\rho_{\rm ds} + \frac{R_{\rm r}}{L_{\rm r}}\right)\tilde{i}_{\rm ds} - \omega_{\rm r}\tilde{i}_{\rm qs}\\ &+ \tilde{\omega}_{\rm r}\left(\zeta_{\rm qs} + \frac{L_{\rm m}}{\sigma L_{\rm s}L_{\rm r}}\hat{\lambda}_{\rm qr}\right) + \tilde{\xi}_{\rm ds} - \frac{\tilde{R}_{\rm s}}{\sigma L_{\rm s}}i_{\rm ds}\\ \dot{\tilde{i}}_{\rm qs} =& \omega_{\rm r}\tilde{i}_{\rm ds} - \left(\rho_{\rm qs} + \frac{R_{\rm r}}{L_{\rm r}}\right)\tilde{i}_{\rm qs}\\ &- \tilde{\omega}_{\rm r}\left(\zeta_{\rm ds} + \frac{L_{\rm m}}{\sigma L_{\rm s}L_{\rm r}}\hat{\lambda}_{\rm qr}\right) + \tilde{\xi}_{\rm qs} - \frac{\tilde{R}_{\rm s}}{\sigma L_{\rm s}}i_{\rm qs}\end{aligned} \tag{32}$$

where $\tilde{R}_{\rm s} = R_{\rm s} - \hat{R}_{\rm s}$.

A Lyapunov function $V_{\rm s}$ is defined as follows:

$$V_{\rm s} = \frac{1}{2}\left(\tilde{i}_{\rm ds}^2 + \tilde{i}_{\rm qs}^2 + \frac{1}{\gamma_1}\tilde{\omega}_{\rm r}^2 + \frac{1}{\gamma_2}\tilde{\xi}_{\rm ds}^2 + \frac{1}{\gamma_3}\tilde{\xi}_{\rm qs}^2 + \frac{1}{\gamma_4}\tilde{R}_{\rm s}^2\right) \tag{33}$$

where γ_4 is a positive design parameter and its time derivative is

$$\begin{aligned}\dot{V}_{\rm s} &= \dot{V} + \frac{\tilde{R}_{\rm s}}{\sigma L_{\rm s}}(i_{\rm ds}\tilde{i}_{\rm ds} + i_{\rm qs}\tilde{i}_{\rm qs}) + \frac{1}{\gamma_4}\tilde{R}_{\rm s}\dot{\tilde{R}}_{\rm s}\\ &= \dot{V} + \frac{\tilde{R}_{\rm s}}{\sigma L_{\rm s}}(i_{\rm ds}\tilde{i}_{\rm ds} + i_{\rm qs}\tilde{i}_{\rm qs}) + \frac{1}{\gamma_4}\tilde{R}_{\rm s}\dot{\hat{R}}_{\rm s}.\end{aligned} \tag{34}$$

The adaptive scheme for stator resistance estimation is founded by equating the second and third term in (34)

$$\dot{\hat{R}}_{\rm s} = -\mu_1(i_{\rm ds}\tilde{i}_{\rm ds} + i_{\rm qs}\tilde{i}_{\rm qs}) \tag{35}$$

where μ_1 is a positive design parameter.

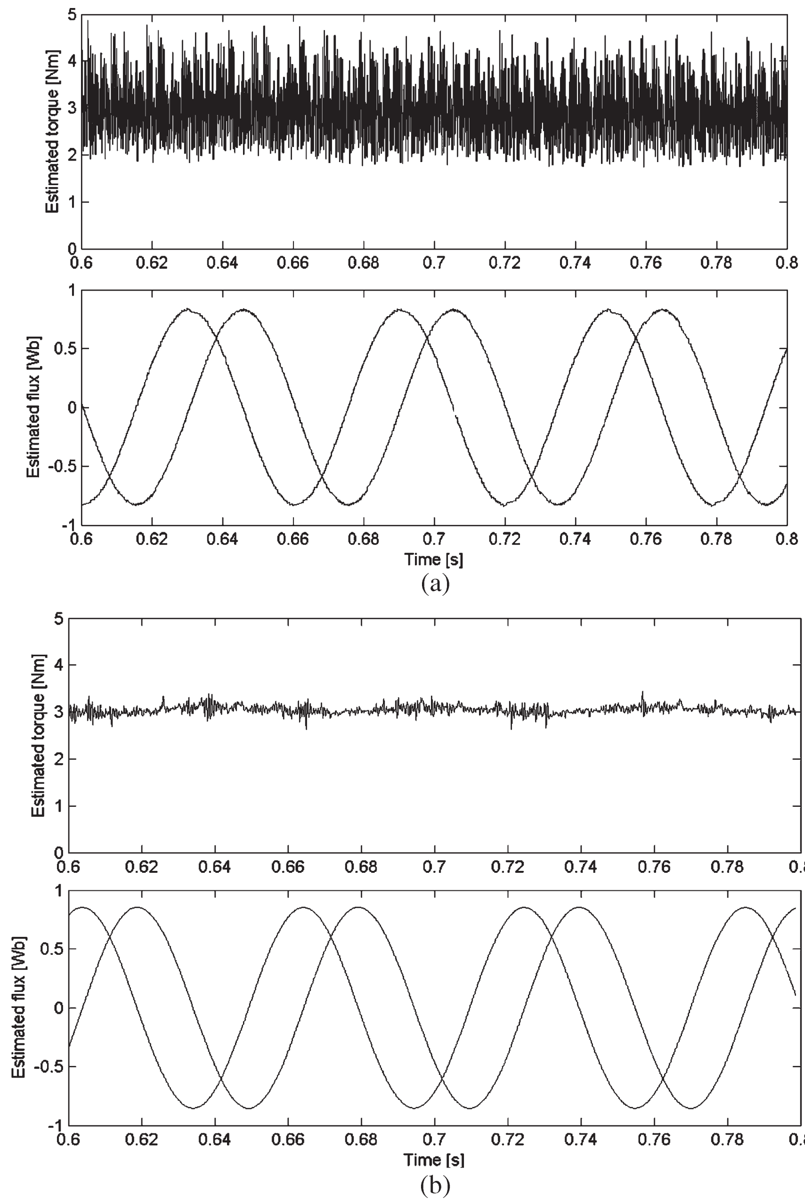

Fig. 8. Estimated torque and estimated flux at 500 r/min with 15% of rated load. (a) Conventional DTC. (b) Proposed DTC.

IV. Experiments

Experiments are carried out to confirm the validity of the proposed observer. The robustness of the speed response against the parameter variation and low speed operation are especially given focus in the experiment. The experimental setup of the proposed control system consists of a three-phase, 380 V, 60 Hz, four pole, 3 kW induction motor and power circuit using a matrix converter. The induction motor has the following parameter values: $R_{\mathrm{s}} = 1.79\ \Omega$, $R_{\mathrm{r}} = 1.8\ \Omega$, $L_{\mathrm{s}} = 167$ mH, $L_{\mathrm{r}} = 174.4$ mH, and $L_{\mathrm{m}} = 160$ mH. A dual controller system consisting of a 32-bit DSP (ADSP 21062) and a 16-bit microcontroller (80C167), in conjunction with a 12-bit A/D converter board, is used to control the matrix converter-based induction motor drive.

Fig. 8(a) and (b) show experimental results of the steady state performance of the conventional DTC and modified DTC at 500 r/min. It can be seen from this result that the torque ripple was reduced drastically by the proposed algorithm. The steady state phase currents and their harmonic spectrums are compared in Fig. 9(a) and (b).

From Fig. 9(a), high distortion in the current can be observed and low order harmonics scattered from fundamental to 4 kHz, which are not desirable. The current waveform of the proposed DTC in Fig. 9(b) is smoother than that of the basic DTC and the dominant harmonics are around 6.5 kHz, which is determined by the SVM sampling period.

Fig. 10 shows the filtered input line current and the corresponding line-to-neutral voltage. The line current is in phase with the voltage, confirming the validity of the control scheme which allows unity input power factor operation.

In Fig. 11, comparison of the torque step responses of the two algorithms showed a larger torque ripple in the basic DTC. In Fig. 11(b), the response time of DTC-SVM with an overmodulation strategy is 0.4 ms, which is almost the same

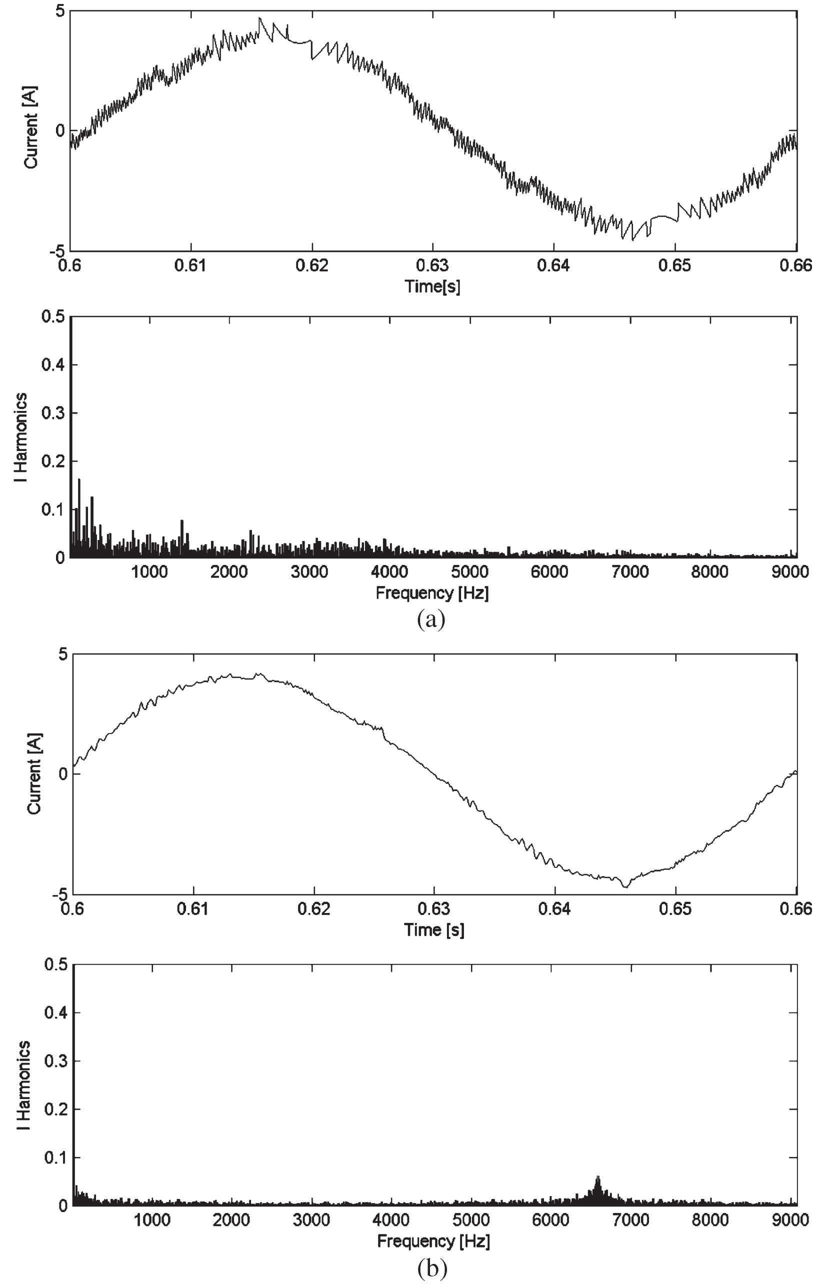

Fig. 9. Phase current and harmonic spectrum at 500 r/min with 15% of rated load. (a) Conventional DTC. (b) Proposed DTC.

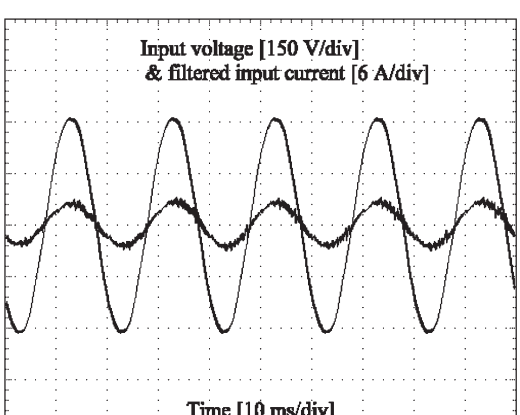

Fig. 10. Input voltage and filtered input current waveform at 1000 r/min.

as that of the basic DTC in Fig. 11(a). Fig. 12 shows the speed and phase current responses of the proposed sensorless vector control system in the forward and reverse operation. It can be seen that the speed response for a ramp-speed reference with a slope is 200 r/min/s. It is noted here that a smooth and stable zero crossing of speed is obtained. Fig. 13 shows the low-speed performance in a speed reversal process between the values ± 50 r/min. The torque is held constant at 40% of rated value such that the drive operates in the generating mode while the speed is negative. Fig. 14 shows speed and phase current responses of the proposed observer-based DTC-SVM, even though the stator resistance increases up to 150% of rated value. The proposed scheme with stator resistance adaptation shows good responses against the parameter variation.

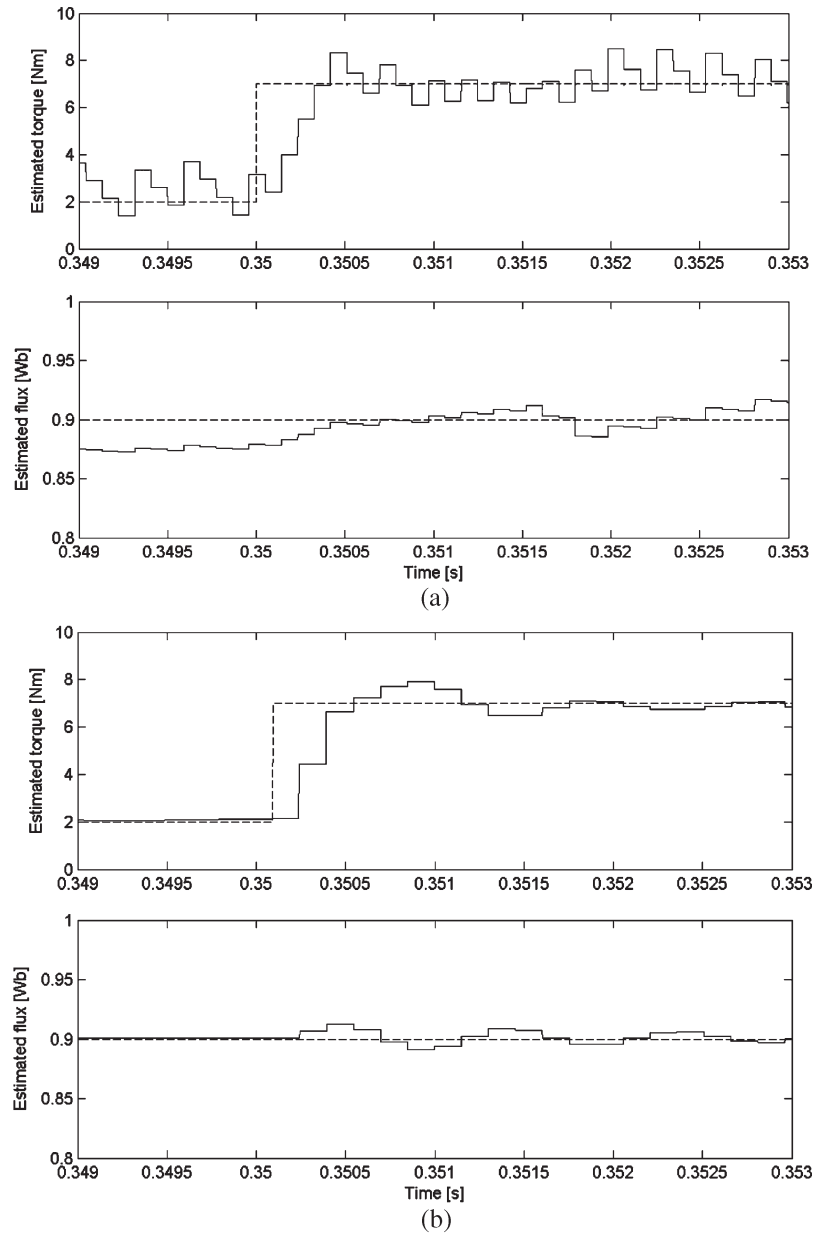

Fig. 11. Torque step responses from 10% to 35% of rated load at 300 r/min (estimated torque and estimated stator flux). (a) Basic DTC. (b) Proposed SVM-DTC with overmodulation strategy.

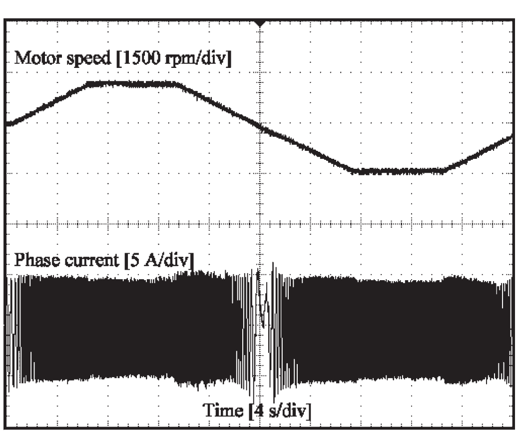

Fig. 12. Forward and reverse operation; speed and phase current.

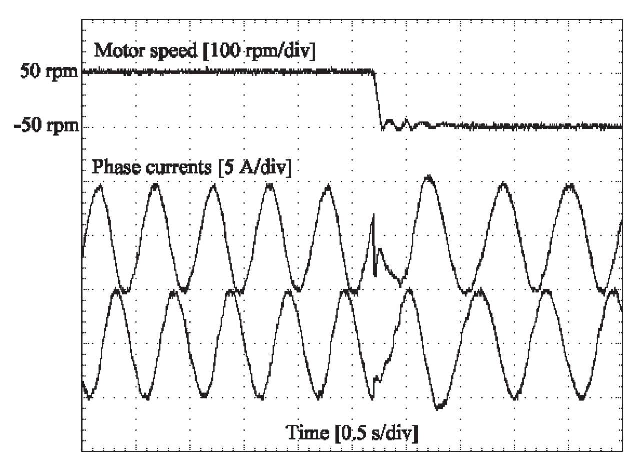

Fig. 13. Reversal speed operation at ± 50 r/min with constant torque (40% rated value).

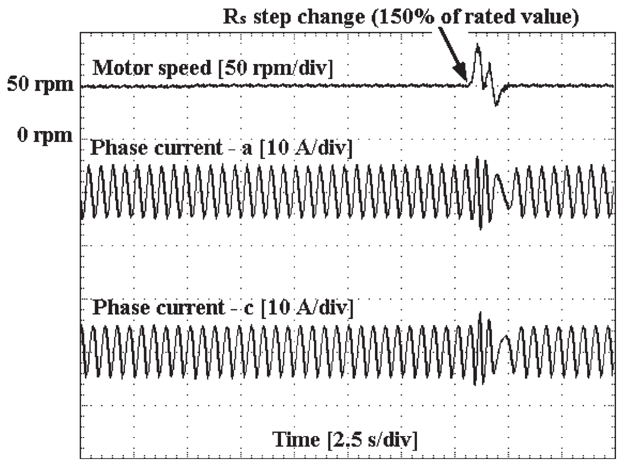

Fig. 14. Response against stator resistance change (150% rated value) at 50 r/min with 30% of rated load.

V. Conclusion

A new and stable sensorless DTC-SVM method for matrix converter drives has been derived and verified with experimental results. The proposed DTC-SVM method using a deadbeat algorithm and an overmodulation strategy helped minimize torque ripple and obtain the unity input power factor, while maintaining constant switching frequency and torque dynamic response. The presented sensorless scheme was independent of the value of the rotor speed. The state estimation problem was converted into a parameter estimation problem assuming that the rotor speed is constant. the stator resistance could also be estimated within the same framework.

References

[1] P. Thoegersen and F. Blaabjerg, "Adjustable speed drives in the next decade: Future steps in industry and academia," *Electr. Power Compon. Syst.*, vol. 32, no. 1, pp. 13–31, Jan. 2004.

[2] M. P. Kazmierkowski, R. Krishnan, and F. Blaabjerg, *Control in Power Electronics—Selected Problems*. New York: Academic, 2002, ch. 3.

[3] D. Casadei, G. Serra, and A. Tani, "The use of matrix converters in direct torque control of induction machines," *IEEE Trans. Ind. Electron.*, vol. 48, no. 6, pp. 1057–1064, Dec. 2001.

[4] K. B. Lee, J. H. Song, I. Choy, and J. Y. Yoo, "Torque ripple reduction in DTC of induction motor driven by three-level inverter with low switching frequency," *IEEE Trans. Power Electron.*, vol. 17, no. 2, pp. 255–264, Mar. 2002.

[5] L. Tang, L. Zhong, M. F. Rahman, and Y. Hu, "A novel direct torque controlled interior permanent magnet synchronous machine drive with low ripple in flux and torque and fixed switching frequency," *IEEE Trans. Power Electron.*, vol. 19, no. 2, pp. 346–354, Mar. 2004.

[6] C. Lascu, I. Boldea, and F. Blaabjerg, "Variable-structure direct torque control—A class of fast and robust controllers for induction machine drives," *IEEE Trans. Ind. Electron.*, vol. 51, no. 4, pp. 785–792, Aug. 2004.

[7] B. H. Kenny and R. D. Lorenz, "Stator- and rotor-flux-based deadbeat direct torque control of induction machines," *IEEE Trans. Ind. Appl.*, vol. 39, no. 4, pp. 1093–1101, Jul./Aug. 2003.

[8] R. Kim, S. K. Sul, and M. H. Park, "Speed sensorless vector control of induction motor using extended Kalman filter," *IEEE Trans. Ind. Appl.*, vol. 30, no. 5, pp. 1225–1233, Sep./Oct. 1994.

[9] M. Hinkkanen, "Analysis and design of full-order flux observers for sensorless induction motors," *IEEE Trans. Ind. Electron.*, vol. 51, no. 5, pp. 1033–1040, Oct. 2004.

[10] H. Kuboda, I. Sato, Y. Tamura, K. Matsuse, H. Ohta, and Y. Hori, "Regenerating-mode low speed operation of sensorless induction motor drive with adaptive observer," *IEEE Trans. Ind. Appl.*, vol. 38, no. 4, pp. 1081–1086, Jul./Aug. 2002.

[11] K. B. Lee, J. H. Song, I. Choy, and J. Y. Yoo, "Improvement of low-speed operation performance of DTC for three-level inverter-fed induction motors," *IEEE Trans. Ind. Electron.*, vol. 48, no. 5, pp. 1006–1014, Oct. 2001.

[12] V. A. Bondarko and A. T. Zaremba, "Speed and flux estimation for an induction motor without position sensor," in *Proc. ACC*, 1999, pp. 3890–3894.

[13] K. B. Lee and F. Blaabjerg, "Improved sensorless vector control for induction motor drives fed by a matrix converter using nonlinear modeling and disturbance observer," *IEEE Trans. Energy Convers.*, vol. 21, no. 1, pp. 52–59, Mar. 2006.

[14] G. S. Lee, D. H. Lee, T. W. Yoon, K. B. Lee, J. H. Song, and I. Choy, "Speed and flux estimation for an induction motor using a parameter estimation technique," *Int. J. Control Autom. Syst.*, vol. 3, no. 1, pp. 79–86, Mar. 2005.

[15] K. B. Lee and F. Blaabjerg, "An improved DTC-SVM method for sensorless matrix converter drives using an overmodulation strategy and a simple non-linearity compensation," *IEEE Trans. Ind. Electron.*, vol. 54, no. 6, pp. 3155–3166, Dec. 2007.

[16] K. B. Lee and F. Blaabjerg, "An improved DTC-SVM method for matrix converter drives using a deadbeat scheme," *Int. J. Electron.*, vol. 93, no. 11, pp. 737–753, Nov. 2006.

Kyo-Beum Lee (S'01–M'04) received the B.S. and M.S. degrees in electrical and electronic engineering from Ajou University, Suwon, Korea, in 1997 and 1999, respectively, and the Ph.D. degree in electrical engineering from Korea University, Seoul, Korea, in 2003.

From 2003 to 2006, he was with the Institute of Energy Technology, Aalborg University, Aalborg, Denmark. From 2006 to 2007, he was with the Division of Electronics and Information Engineering, Chonbuk National University, Jeonju, Korea. In 2007, he joined the School of Electrical and Computer Engineering, Ajou University. His research interests include electric machine drives, power electronics, and wind power generations.

Dr. Lee received two IEEE Prize Paper Awards.

Frede Blaabjerg (S'90–M'91–SM'97–F'03) was born in Erslev, Denmark, on May 6, 1963. He received the M.Sc.E.E. and Ph.D. degrees from Aalborg University (AAU), Aalborg, Denmark, in 1987 and 1995, respectively.

He was employed at ABB-Scandia, Randers, from 1987 to 1988. In 1992, he became an Assistant Professor at AAU, an Associate Professor in 1996, and Full Professor in power electronics and drives in 1998. He is the Author or Coauthor of more than 300 publications in his research fields including the book *Control in Power Electronics* (New York: Academic, 2002).

Dr. Blaabjerg received the 1995 Angelos Award for his contribution in modulation technique and control of electric drives, and the Annual Teacher prize at AAU, in 1995. In 1998, he received the Outstanding Young Power Electronics Engineer Award from the IEEE Power Electronics Society. He has received four IEEE Prize paper awards during the last five years. In 2002, he received the C.Y. O'Connor fellowship from Perth, Australia, the Statoil-prize in 2003 for his contributions in Power Electronics, and the Grundfos-prize in 2004 for his contributions in power electronics and drives. He is the Editor of the IEEE Transactions on Industry Applications, and Associate Editor of the IEEE Transactions on Power Electronics, *Journal of Power Electronics* and of the Danish journal *Elteknik*. He has held a number of chairman positions in research policy and research funding bodies in Denmark.